ARTICLE
Journal of Cellular Biochemistry 105:905–912 (2008)

Journal of Cellular Biochemistry

CD38 Is Constitutively Expressed in the Nucleus of Human Hematopoietic Cells

M. Orciani,[1] O. Trubiani,[2] S. Guarnieri,[3,4] E. Ferrero,[5] and R. Di Primio[1*]

[1]*Department of Molecular Pathology and Innovative Therapies, Histology Section, Marche Polytechnic University, Ancona, Italy*

[2]*Department of Stomatology and Oral Science, "G. D'Annunzio" University, Chieti, Italy*

[3]*Department of Basic and Applied Medical Science, Institute of Myology, "G. D'Annunzio" University, Chieti, Italy*

[4]*Clinical Research Center CRC-CeSI, "G. D'Annunzio" University Foundation, Chieti, Italy*

[5]*Laboratory of Immunogenetics, Department of Genetics, Biology & Biochemistry, University of Torino, CeRMS, Turin, Italy*

ABSTRACT

CD38 is a type II glycoprotein that acts both as a bifunctional enzyme, responsible for the synthesis and hydrolysis of cyclic ADP-ribose, and as a signal-transducing surface receptor. Although CD38 was originally described as a plasma membrane molecule, several reports indicate that CD38 is expressed in the nucleus, even in cells known to be CD38 surface-negative. In this study, firstly we investigated the presence of nuclear CD38 by immunofluorescence and confocal microscopy using a panel of hematopoietic cell lines that exhibit different levels of CD38 plasma membrane expression. Our second aim was to explore the relationship between the nuclear and plasma membrane forms of CD38 in human cell lines which represent discrete early maturation stages of the human lymphoid and myeloid compartments. Our results indicate that CD38 is constitutively present in the nucleus of cells belonging to distinct lineages. Furthermore, nuclear CD38 appears to be independent of the plasma membrane pool. The presence of nuclear CD38 during different stages of hematopoietic differentiation suggests that it may play a role in the control of nuclear Ca^{2+} homeostasis and NAD levels. J. Cell. Biochem. 105: 905–912, 2008.

KEY WORDS: CD38; NUCLEUS; HEMOPOIESIS; CADPR

Human CD38 is a 45-kDa type II glycoprotein that was originally described as a lymphoid cell surface differentiation marker [Kung et al., 1979]. First identified functionally as a receptor [Funaro et al., 1990], CD38 subsequently gained recognition as a complex ectoenzyme [Lee, 2006] with NAD^+ glycohydrolase and ADP-ribosyl cyclase activities. Cyclic ADPR (cADPR), the intermediate product, is a potent Ca^{2+} mobilizing agent, which acts independently of inositol 1,4,5-trisphosphate [Lee, 1997]. The CD38 gene maps to chromosome 4p15 [Katz et al., 1983] and shares a long evolutionary history with CD157 [Hirata et al., 1994], a second mammalian member of the ADP-ribosyl cyclase family that also maps to 4p15 [Ferrero et al., 1999]. Both CD38 and CD157 genes maintain a close structural similarity to homologs in *Aplysia*, chicken, rodents, and cynomolgus monkey [Malavasi et al., 2006]. Both genes are also characterized by complex regulatory regions, only partially defined in functional terms [Ferrero et al., 1999].

The study of CD38 as a receptor and ectoenzyme has been carried out primarily in hematopoietic cells, in human and murine models [Lund, 2006], with somewhat discordant results. Other open questions concerning CD38 include its tissue distribution and subcellular compartmentalization. Current assessment of the tissue distribution of CD38 is still heavily influenced by its initial definition as a leukocyte molecule; however, we now know that CD38 is widely expressed outside the hematological and immunological districts [Adebanjo et al., 2000]. The intracellular localization of the molecule is instead currently under investigation. Detection of CD38 in the nucleus of mammalian cells was reported by Adebanjo et al. [1999] and Khoo and Chang (2002), and we previously described CD38 expression within the nucleoplasm [Trubiani et al., 2007]. Taken together, these results prompt speculation that the physiological role of nuclear CD38 may be to interact with ryanodine receptors (RyRs) localized in the inner nuclear membrane.

Grant sponsor: Università Politecnica delle Marche Research Grant (2008).

*Correspondence to: R. Di Primio, Department of Molecular Pathology and Innovative Therapies, Histology Section, Marche Polytechnic University, Via Tronto 10/A, 60020 Ancona, Italy. E-mail: r.diprimio@univpm.it

Received 27 May 2008; Accepted 17 July 2008 • DOI 10.1002/jcb.21887 • 2008 Wiley-Liss, Inc.
Published online 29 August 2008 in Wiley InterScience (www.interscience.wiley.com).

Our working hypothesis is that CD38 contributes to the generation of cADPR inside the nucleus, which in turn activates the inner nuclear membrane RyRs leading to Ca^{2+} flux into the nucleoplasm. Our approach was firstly to obtain a clear description of CD38 expression in the nucleus through careful evaluation of its distribution, regulation and relationship with the CD38 fraction expressed on the plasma membrane. The experimental models we adopted were human lymphoid and myeloid cell lines, and peripheral blood mononuclear cells (PBMC) from healthy donors as normal controls. Regulation of nuclear CD38 was assessed by treating cell lines with growth factors and drugs known to influence CD38 expression on the cell surface.

MATERIALS AND METHODS

CELLS

The human cell lines used in this work are: (i) RPMI-8402, a $CD38^+/TdT^+$ pre-T cell leukemia (DMSZ, Braunschweig, Germany; (ii) Daudi, a $CD38^+/TdT^-$ Burkitt's lymphoma, (DSMZ); (iii) U937, a $CD38^+/TdT^-$ M4 histiocytic lymphoma (ATCC, Manassas, VA); (iv) HL60, a $CD38^{+/-}/TdT^-$ M2 promyelocytic leukemia, (ATCC); (v) NB-4, a $CD38^+/TdT^-$ M3 promyelocytic leukemia (DSMZ); (vi) Mono-Mac-6, a $CD38^+/TdT^-$ M5 acute monocytic leukemia (DSMZ) and (vii) K562, a $CD38^-/TdT^-$ M6 erythroleukemia cell line (ATCC). These cell lines were selected as they represent different steps of hematopoietic differentiation, and they vary in their expression levels of membrane CD38.

Peripheral blood from normal healthy donors was layered over Ficoll-Hypaque and centrifuged at 400*g* for 20 min. Mononuclear cells (PBMC) were harvested at the interface and washed with PBS.

ANTIBODIES

The anti-CD38 mAbs used were: IB4 (IgG_{2a}), SUN-4B7 (IgG_1) and AT1 (IgG_1). These mAbs recognize discrete epitopes of the CD38 ectodomain [Hoshino et al., 1997; Ausiello et al., 2000; Ferrero et al., 2004]. mAb binding experiments were performed in sequence, first adding IB4 followed by AT1 or SUN-4B7 mAbs to rule out aspecific binding, the role of antibody isotype and their receptors. All mAbs were produced and purified in-house [Horenstein et al., 2003]. Anti-Terminal Deoxynucleotidyl Transferase (TdT) and anti-HLA Class I mAbs were purchased from Sigma (Milano, Italy). Goat anti-mouse Ig labeled with fluorescein isothiocyanate anti-serum (GaMIg-FITC) was from ImmunoTools (Friesoythe, Germany). The rabbit polyclonal anti-human p80-coilin anti-serum, the goat anti-rabbit IgG antibody labeled with Texas Red (GaRIg-TR) and the goat anti-mouse Ig antibody labeled with horseradish peroxidase (GaMIg-HRP) were purchased from Santa Cruz Biotechology (Santa Cruz, CA).

NUCLEAR PREPARATION

Nuclei were obtained from cells and cell lines as previously described [Trubiani et al., 2000]. In detail, growing cells were washed in PBS, incubated for 10 min at 10°C in a solution containing 2 mM $MgCl_2$, 1 mM phenylmethylsulfonyl fluoride (PMSF) and 10 mM Tris–HCl, pH 7.4, and then treated with Triton X-100 (0.3% final concentration). Cell suspensions were passed twice through a syringe with a 20 gauge needle, and $MgCl_2$ adjusted to a final concentration of 5 mM. Partially lysed cells were resuspended in cold hypotonic lysis buffer. Protein concentration was determined by colorimetric assay (Bio-Rad, Milano, Italy).

IMMUNOFLUORESCENCE STAINING (IIF) AND CONFOCAL LASER SCANNING MICROSCOPY

Cell lines (both intact and permeabilized forms) and nuclei isolated from them were treated with the anti-CD38 mAbs and incubated with GaMIg-FITC. For permeabilization, cells were treated with Triton X-100 (0.1% final concentration). Positive control staining for isolated nuclei was detection of TdT, while staining with anti-HLA Class I mAb was used as negative control. Following incubation with GaMIg-FITC, samples were treated with 0.1% propidium iodide (PI) for 10 min and visualized by means of a ZEISS LSM510 META confocal microscope (Jena, Germany) equipped with an argon laser. Double immunostaining to confirm co-expression of CD38 and p80-coilin were obtained using mouse anti-human CD38 followed by GaMIg-FITC, and rabbit polyclonal anti-human p80-coilin anti-sera followed by GaRIg-TR, respectively.

WESTERN BLOTTING

Purified nuclear and total cellular lysates were obtained from untreated cell lines and leukocytes, and from treated HL60 and K562 cells. Lysates were separated on 12% polyacrylamide–SDS gels and transferred by electrophoresis to a polyvinylidene fluoride (PVDF) membrane. After blocking, the membrane was incubated overnight at 4°C with the primary anti-CD38 mAb (IB4, 3 μg/ml), washed and then probed with GaMIg-HRP diluted in Tris-buffered saline-Tween-20 (TBST, 1:10,000) at room temperature for 1 h. After washing, the proteins on the membrane were visualized by chemiluminescence. Nuclear purity was assessed by detection of β-tubulin: only nuclear preparations showing a complete absence of β-tubulin by Western blot were used in the reported experiments. Pre-stained SDS–PAGE standard protein markers (Sigma) was loaded to calibrate molecular masses.

RNA ISOLATION AND RT-PCR ANALYSIS

Total RNA was isolated from 5×10^6 cells using the SV Total RNA Isolation Systems (Promega, Milano, Italy) according to the manufacturer's instructions. Total RNA (1.5 μg) was reverse-transcribed with 1.25 μM of oligo $d(T)_{16}$ using ImProm-II™ Reverse Transcriptase (Promega). PCR amplification of cDNA was performed using intron-spanning primers (Invitrogen, Milano, Italy) to avoid genomic DNA contamination; β-actin: forward 5′-CCAACCGCGA-GAAGATGAC-3′; reverse: 5′-GAGGCGTACAGGGATAGCACA-3′; CD38: forward 5′-AGACTGCCAAAGTGTATGGGAT-3′; reverse: 5′-GG AAGTGTTGAATTCACCACAC-3′). Reactions were performed in a DNA thermal cycler having previously established the PCR cycle number required for each primer pair (26 for β-actin and 38 for CD38) to prevent plateau effects. β-actin was used as an internal standard. Each amplification product was run on a 2% agarose gel stained with ethidium bromide and quantified by densitometry using a KODAK EDAS 290 densitometer and a KODAK 1D Image Analysis Software (Rochester, NY). The expression of each specific

gene is indicated as the ratio of the intensities of specific transcripts to those of β-actin.

ACTIVATION AND APOPTOSIS

K562 and HL60 cells were treated for 48 h with 100 nM phorbol 12-myristate 13-acetate (PMA) (Sigma) and 1 μM all-*trans* retinoic acid (ATRA) (Sigma). The effects of the treatments [Drach et al., 1993; Kishimoto et al., 1998] were confirmed by monitoring the levels of membrane CD38. To analyze CD38 distribution throughout the cell cycle, RPMI-8402, Daudi and K562 cells were synchronized by complete serum depletion for 48 h and then cultured in the presence of 4% FCS to re-enter the cell cycle. Apoptosis was evaluated by fluorescence microscopy after staining cells with ethidium bromide/acridine orange solution. Cells were scored as either viable or non-viable, and either normal or apoptotic. Apoptosis was also evaluated by electron microscopy. Analysis was performed by fixing cell pellets with 2.5% glutaraldehyde in 0.1 M cacodylate buffer, pH 7.4, and then post-fixing them in 1% OsO_4 in cacodylate buffer, ethanol dehydrated and embedded in araldite. Thin sections stained with uranyl acetate and lead citrate were analyzed with a Philips CM10 electron microscope at 80 kV (Eindhoven, The Netherlands). Programmed cell death was triggered in RPMI-8402 cells [Trubiani et al., 2003] with 1.5% (v/v) dimethyl sulfoxide (DMSO) (Sigma) for 48 h; in Daudi cells [Di Pietro et al., 1997] with 1 μg/ml tumor necrosis factor α (TNF-α) (Sigma) for 12 h; and in HL-60 cells (Shimizu and Pommier, 1997) with 0.15 M camptothecin (Campto) (Sigma) for 8 h, respectively.

EVALUATION OF GDP-RIBOSYL CYCLASE ACTIVITY

The cyclase activity of CD38 in the selected cell lines was evaluated by incubation with nicotinamide guanine dinucleotide (NGD^+) (Sigma), an NAD^+ analogue which is converted to cyclic GDPR (cGDPR). Unlike cADPR, cGDPR is a fluorescent and cell impermeant end-product, detectable in supernatants. Briefly, isolated nuclei or intact cells were resuspended in NGT buffer (0.15 M NaCl, 5 mM glucose, 10 mM Tris–HCl, pH 7.4). Triton X-100 at a 0.1% final concentration was used to permeabilize cells. Ten microliters of 10 mM NGD^+ in 20 mM Tris–HCl, pH 7.4, or 10 μl control buffer were added to the nuclear and cellular suspensions. After 30 min at 37°C, supernatants were collected after brief centrifugation. The conversion of NGD^+ to the fluorescent cGDPR end-product in supernatants was evaluated by means of a fluorescence spectrometer (Perkin-Elmer, Boston, MA), set at 300 nm excitation wavelength and 410 nm emission wavelength.

EVALUATION OF INTRACELLULAR AND INTRANUCLEAR Ca^{2+} CONCENTRATION

Intracellular and intranuclear Ca^{2+} concentration was measured using intact cells and isolated nuclei loaded with the fluorescent probe FURA 2-AM (Invitrogen) [Grynkiewicz et al., 1985]. Measurements were performed at 37°C using a Perkin-Elmer LS 50 B spectrofluorometer according to the method described by Rao [1988]. Fluorescence intensity was evaluated at a constant emission wavelength (490 nm) with changes in the excitation wavelength (340 and 380 nm). At the end of each experiment, the higher and the lower fluorescence values obtained at each excitation wavelength were obtained after lysing the cells with 0.1% Triton X-100 (top) and then adding 10 mM EGTA (low). The top and low reference scores allowed conversion of the 340/380 nm fluorescence ratios in free Ca^{2+} concentrations, exploiting the FURA 2-AM Ca^{2+} binding constant (135 nM) and the formula reported by Grynkiewicz et al. [1985].

RESULTS

Nuclear CD38 was investigated in a panel of hematopoietic cell lines, selected because they express different levels of surface CD38, varying from high to low to nil: RPMI-8402 (pre-T cell leukemia, surface $CD38^+$), Daudi (Burkitt's lymphoma, surface $CD38^+$), U937 (M4 histiocytic lymphoma, surface $CD38^+$), HL60 (M2 promyelocytic leukemia, surface $CD38^+$), NB-4 (M3 promyelocytic leukemia, surface $CD38^+$), Mono-Mac-6 (M5 acute monocytic leukemia, surface $CD38^+$), and K562 (M6 erythroleukemia cell line, surface $CD38^-$). Cells were also analyzed in resting, proliferating and apoptotic conditions. CD38 was detected by means of mAbs recognizing discrete epitopes of the molecule. Anti-TdT and anti-HLA mAbs were used in immunochemistry as background controls.

ANALYSIS OF CD38 SUBCELLULAR LOCALIZATION IN HUMAN LYMPHOID AND MYELOID CELLS

Nuclei, intact cells and permeabilized cells were analyzed by indirect immunofluorescence (IIF) with anti-CD38 mAbs to detect the presence and compartmentalization of CD38 by confocal microscopy. PMBC from healthy donors were used as reference controls. In nuclei isolated from RPMI-8402, Daudi and K562, CD38 was distributed diffusely or in punctate bodies which varied in number and shape (Fig. 1, section A). These results indicate that this pattern is common to the pre-T, B and myeloid cell lines tested here. The diffuse reticular pattern is similar to the distribution of chromatin while the punctate body morphology is strongly reminiscent of micronuclei (also known as Cajal bodies) [Gall, 2003; Platani and Lamond, 2004].

To investigate the presence of CD38 in Cajal bodies, nuclei were stained simultaneously with an antibody directed against coilin (a signature marker of Cajal bodies) followed by texas red-labeled secondary antibody, and anti-CD38 followed by GaMIg-FITC. The merged images demonstrate that CD38 and coilin co-localized in nuclear bodies (Fig. 1, section B). To exclude the possibility of artifactual results, nuclear preparations were analyzed for the presence of TdT and the lack HLA Class I, while CD38 expression was detected using either IB4 or AT-1 anti-CD38 mAbs specific for separate epitopes (Fig. 1, section C). To address the possibility of antibody cross-reactivity with other molecules sharing epitopes with CD38, we performed Western blot and PCR experiments. Expression of CD38 and TdT proteins was analyzed in nuclei isolated from three representative cell lines: (1) RPMI-8402, which is surface $CD38^+/TdT^+$; (2) Daudi, which is surface $CD38^+/TdT^-$ and (3) K562, which is negative for both surface CD38 and nuclear TdT. Anti-CD38 mAbs detected a 43 kDa band of similar intensity in nuclei derived from all three cell lines (Fig. 2, panel A). To control for nuclear fraction purification, membranes were stripped and probed with anti-TdT mAb which, as expected, identified a band only in the RPMI-8402 TdT^+ cell line (Fig. 2, section A).

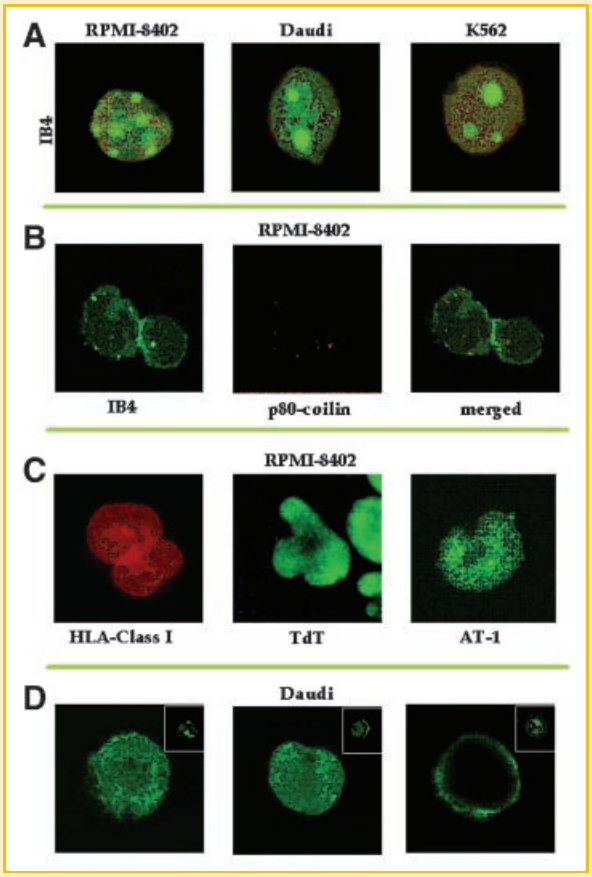

Fig. 1. A: Fluorescent staining of CD38 from nuclei isolated from RPMI-8402, Daudi and K562 cells. Nuclei were recovered from intact and permeabilized cells, stained with anti-CD38 mAbs and counterstained with a 0.1% PI solution to detect the presence and compartmentalization of the molecule by confocal microscopy. CD38 shows a punctate distribution; (B) confocal microscopic demonstration that CD38 and p80-coilin co-localize in nuclear preparations obtained as above from RPMI-8402. Green: CD38-FITC; Red: p80-coilin-Texas Red; (C) controls used in confocal microscopy experiments: the presence of TdT in nuclei and the simultaneous absence of HLA Class I molecules prove that the presence of CD38 is not artifactual, as confirmed also by the binding of AT-1, another anti-CD38 antibody. D: IIF staining of CD38 from nuclei isolated from Daudi cells. Samples were incubated with AT1 (anti-CD38) mAb followed by GaMIg-FITC antibody. CD38 distribution is variable, ranging from a homogeneous to a more condensed localization, and to discrete ring-like shapes. The inserts show the CD38 staining in the whole permeabilized cells.

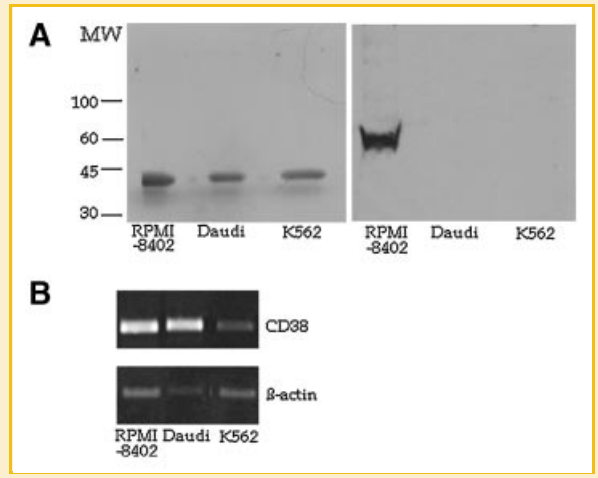

Fig. 2. A: CD38 (left) detection by WB in nuclei isolated from RPMI-8402 (lane 1), Daudi (lane 2), and K562 (lane 3) cells. The membrane was then stripped and re-probed with anti-TdT antibody (right) as control experiment of the nuclear purification. MW: molecular weight. B: Ethidium bromide-stained 2% agarose gel showing cDNA amplification by RT-PCR of CD38 and β-actin (lower line) from RPMI-8402, Daudi and K562 cells.

CD38 mRNA was analyzed by semiquantitative RT-PCR after 38 cycles of amplification (Fig. 2, section B). Quantitative evaluation of expression was determined as the ratio between the intensities of the CD38 versus the β-actin amplification band, and yielded different values according to the cell line. CD38 mRNA levels were highest in Daudi and RPMI-8402 cells, while the lowest value was observed in K562.

VARIABILITY OF CD38 DISTRIBUTION PATTERN IN NUCLEI DERIVED FROM HUMAN HEMATOPOIETIC CELLS

The results of this work add to our preceding observations of nucleoplasmic CD38, demonstrating that the CD38 expression pattern varies from homogeneous distribution to a more condensed localization, to discrete ring-like shapes (Fig. 1, section D). We hypothesized that the pattern adopted by nuclear CD38 might change in response to events occurring in the cell, such as activation and apoptosis. The effects of activation on nuclear CD38 was analyzed in cells synchronized following serum starvation (Fig. 3, section A). RPMI-8402, Daudi and K562 lines were cultured for 48 h in the absence of fetal calf serum and then incubated in the presence of 4% FCS to re-induce cell cycle progression. Following treatment, nuclei were recovered and CD38 expression evaluated by IIF and confocal microscopy (Fig. 3, panel B). CD38 was homogeneously distributed in a significant portion (50–60%) of the nuclei observed, while it was partially condensed or clustered into discrete compartments in ~30% of the nuclei. The remaining 10–20% of the nuclei were characterized by a ring-like localization of CD38, apparently linked to the inner nuclear membrane. As described above, Cajal bodies were found to contain CD38, but they lacked CD38 when the nuclei were derived from synchronized cells. This finding, made using tumor cell lines, was confirmed in PBMC, a normal cellular counterpart selected as a model because of their easy accessibility and because they include T, B and myeloid cells. The results obtained are strikingly similar to those obtained using the continuous cell lines. A reasonable conclusion is that nuclear CD38 localization is independent from lineage and differentiation and almost identical in normal and leukemic cells. In the same experiments, whole cells were used to detect the distribution of CD38 on the cell membrane during the cell cycle; as expected by our previous observations, the plasma membrane pool appears to be independent of cell activation (inserts in Fig. 3, section B).

Next, we examined CD38 in the nuclei of apoptotic cells, induced in RPMI-8402 by DMSO, in Daudi by TNF-α and in K562 by camptothecin. After induction of apoptosis (Fig. 3, panel C, image a), cells were stained with an anti-CD38 mAb followed by GaMIg-FITC and PI solution (Fig. 3, panel C). CD38 expression was evaluated in

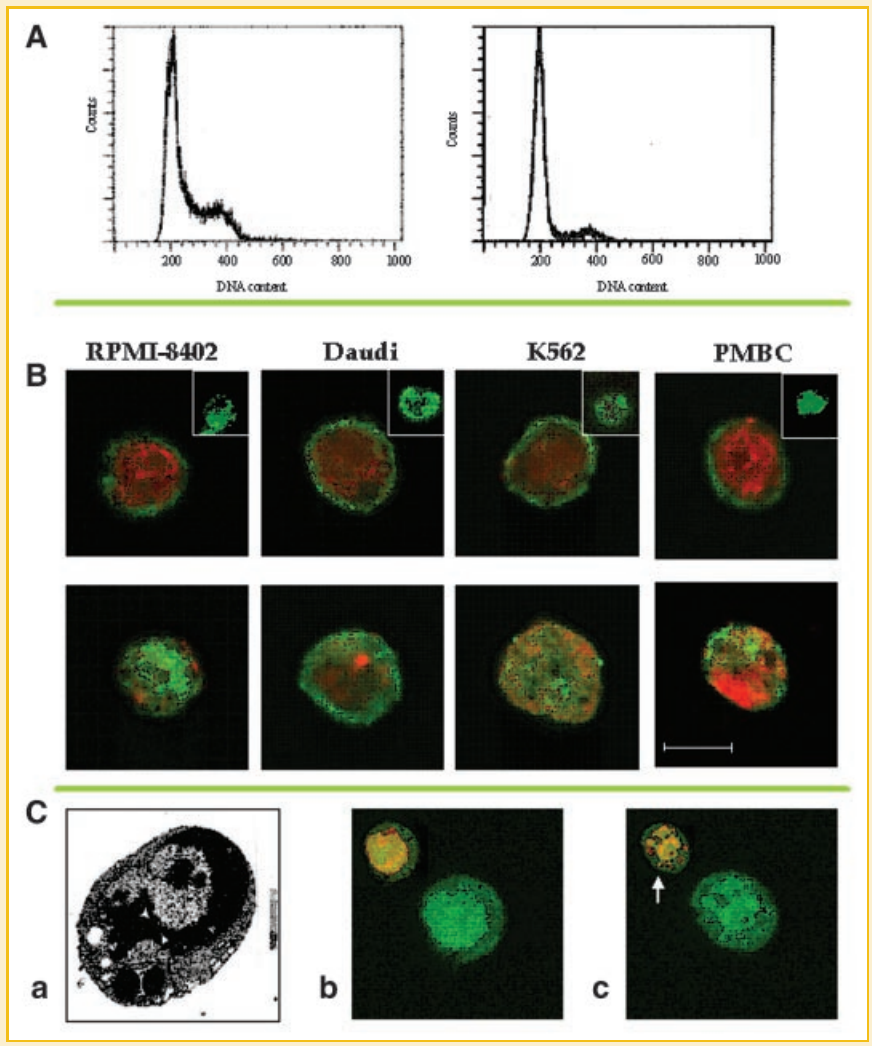

Fig. 3. A: Cell cycle distribution of synchronized evaluated by PI staining and FACS analysis before (left) and after (right) serum starvation. B: CD38 stained in cells synchronized after starvation. Nuclei from RPMI-8402, Daudi, K562 cells and human lymphocytes were treated with AT1 mAb followed by GaMIg-FITC antibody and 0.1% PI solution. Each cell line is analyzed by two merged pseudo-colored overlay images, representing different phases of the cell cycle. Inserts show CD38 distribution in permeabilized whole cells. Bar: 5 μm. C: Section a: morphological analyses by electron microscopy of apoptotic RPMI-8402 cells, showing typical cytoplasmic and nuclear modifications. Sections b and c show the intracellular localization of CD38 in RPMI-8402 cells in early and late apoptosis, respectively. Samples were treated with anti-CD38 mAb directly labeled with FITC and stained with PI. Inserts show merged stainings. Arrows indicate cells at the same apoptotic stage analyzed by different techniques. Bar: 5 μm.

early (Fig. 3, panel C, image b) and late (Fig. 3, panel C, image c) steps of apoptosis. CD38 was detected in the nucleus and in the cytoplasm. The observation of CD38 in the cytoplasm may be due to inhibition of nuclear translocation and to the release from nuclear compartments, for example, from Cajal bodies. The inserts show merged images of PI and FITC labeling. CD38 distribution followed the morphological apoptotic changes, that is, condensation of chromatin at the nuclear periphery, disassembly of nuclear scaffold proteins, and the formation of apoptotic bodies. CD38 was associated with condensed chromatin in apoptotic bodies (arrows).

PHARMACOLOGICAL MODULATION OF CD38 IN DIFFERENT LINEAGES

As CD38 expression is most affected by pharmacological agents in myeloid cell lines, we used K562 and HL60 cells treated, respectively, with 100 nM PMA and 1 μM ATRA, treatments which significantly increase surface expression of CD38. Isolated nuclei and intact cells were then analyzed by Western blot to detect CD38. A band of ~43 kDa was apparent in K562 and HL60 nuclei and in cells treated with PMA and ATRA (Fig. 4, section A) The band from K562 and HL60 nuclei displayed the same intensity before (lanes 1–2) and after (lanes 3–4) differentiating treatments. These observations indicate that the nuclear protein is not inducible with ATRA and PMA. Conversely, the pharmacological effects were visible in the plasma membrane fraction, where increased intensity of the CD38 bands was observed by Western blot (lanes 5–6 vs. 7–8) and IIF (not shown).

CD38 modulation analysis was also performed using PCR. The upper panel contains the bands from CD38 amplification, the lower represent β-actin (Fig. 4, section B). Expression, calculated as the

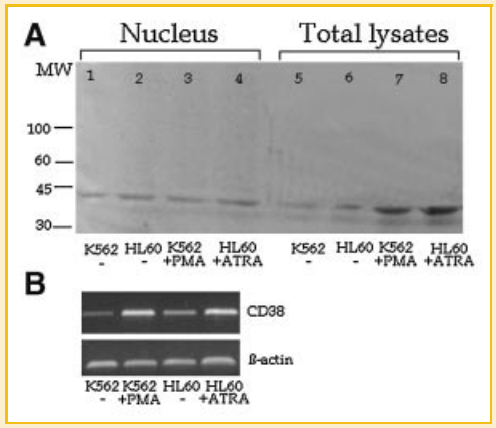

Fig. 4. A: CD38 expression analyzed by WB in K562 and HL60 cells before and after differentiation-inducing treatments. A band of ~43 kDa is detectable in nuclei from untreated K562 and HL60 cells (lanes 1–2), with the same intensity as that observed in nuclei from treated cells (lanes 3–4). The pharmacological effects are visible at a cell membrane level: the immuno-reactive bands in untreated K562 and HL60 cells are less apparent than after treatment (lanes 5–6 vs. 7–8). B: Relative amounts of CD38 mRNA in treated and untreated K562 and HL60 cells determined by RT-PCR. The upper panel displays the bands from CD38 amplification, the lower refers to that of β-actin.

ratio between the intensities of CD38 versus β-actin amplification bands, reveals that PMA and ATRA induce a significant increase of CD38 mRNA levels in K562 and HL60 cells, indirectly confirming the observations derived from WB and IIF.

NUCLEAR CD38 IS ENZYMATICALLY ACTIVE

ADP-ribosyl cyclase activity was measured in isolated nuclei, in intact cells and in permeabilized cells, by assessing the production of cGDPR from the substrate NGD^+. Production of cGDPR was detected in nuclei isolated from all selected cell lines and was quantitatively comparable in all samples (Fig. 5, section A). With the exception of K562, the highest values of cyclase activity were observed following permeabilization, with nuclear and plasma membrane CD38 contributing to the formation of cGDPR. The enzymatic activity of nuclei isolated from K562 cells was almost the same as that of intact cells, indirectly confirming that nuclear CD38 was the only source of cGDPR. The production of cGDPR by nuclear CD38 was not influenced by exposing donor cells to ATRA and PMA as the results obtained with nuclei from untreated and treated cells are highly similar. Conversely, cGDPR production in intact cells was significantly increased by ATRA and PMA treatment, paralleling the upregulation of surface CD38.

INTRACELLULAR AND INTRANUCLEAR Ca^{2+} CONCENTRATION

Using a broad panel of hematopoietic cells characterized by marked differences in membrane expression of CD38, we measured Ca^{2+} concentrations in isolated nuclei and in intact cells using the fluorescent probe FURA 2-AM (Fig. 5, panel B). Nuclear Ca^{2+} levels were found to be uniformly low and not affected by either ATRA or PMA treatment. In these cells, low intranuclear Ca^{2+} levels paralleled the low intranuclear cyclase activity described above.

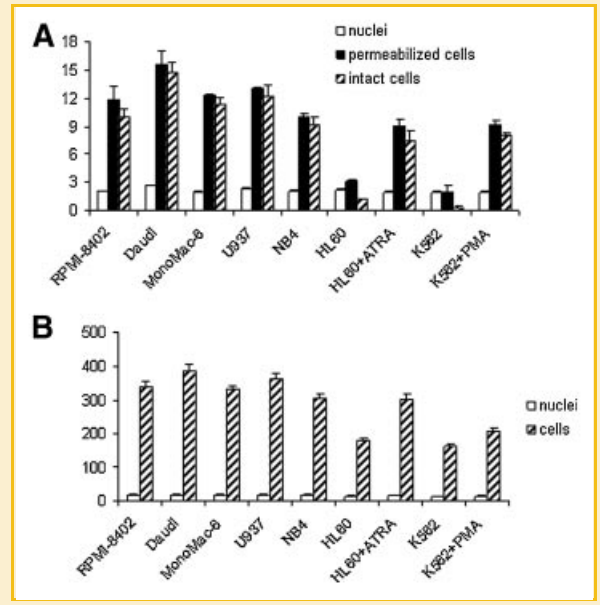

Fig. 5. Detection of ADP-ribosyl cyclase activity and intracellular Ca^{2+} concentration. A: The cyclase activity, measured by assessing the production of fluorescent cGDPR from the substrate NGD^+, is detectable in isolated nuclei from all selected cell lines and is quantitatively comparable in all samples. The indicated fluorescence was calculated as the difference between the values observed in with and without NGD^+ for each preparation. Results shown are representative of three separate experiments. B: Ca^{2+} concentration was tested in isolated nuclei and in intact cells using the fluorescent probe FURA 2-AM. Ca^{2+} levels are almost similar in nuclei derived from cells exhibiting marked differences in surface CD38 expression and are independent from ATRA and PMA treatments.

The intracellular Ca^{2+} levels were instead higher and changed significantly in response to ATRA and PMA.

DISCUSSION

The results of this work clearly indicate that CD38, a type II membrane glycoprotein characterized by plasma membrane localization, is also constitutively localized in the nucleus of human lymphoid and myeloid cells. This result confirms the observations of nuclear CD38 made by others in rodent and human cells. The solid technical approach adopted here to determine the nuclear localization of CD38 is based on the use of a panel of mAbs reacting with discrete epitopes of CD38 and fluorescence confocal microscopy. It provides new evidence that the plasma membrane and nuclear pools of CD38 are distinct and apparently controlled by different regulatory systems, although both exhibit the canonical enzymatic activities.

Results of morphological evaluation indicate that CD38 is finely distributed throughout the nucleus in quiescent cells, where it is often organized in punctate structures that correspond to Cajal bodies, based on coilin co-localization. The function of these structures is currently under investigation. Dundr et al. [2004], for example, have hypothesized that CBs are involved in mechanisms of

compartment-specific retention of proteins. The present results seem to support this hypothesis, and CD38 may be one of the proteins stored in CBs, at least in resting conditions. Indeed, following serum starvation, re-entry into the cell cycle was characterized by significant modifications in the nuclear CD38 localization pattern with loss of uniform distribution followed by clear labeling of CD38 in aggregates and ring-like shapes. These differences suggest that changes in CD38 localization may occur in response to events taking place in the nucleus during cell cycle phases. The reticular network pattern of CD38 is dominant during the G0/G1 phase, while aggregated forms apparently mark the G2 phase. The ring-like structures seem to coincide with early prophase, when the highly condensed nucleus initiates dissolution of its membrane. A further observation is that the nuclear organization of CD38 in apoptotic cells parallels the morphological changes typical of programmed cell death, with CD38 in apparent contact with the nuclear membrane until its dissolution.

Nuclear CD38 was analyzed in structure and function. By Western blot, nuclear CD38 always appeared as a single chain of 43 kDa in reduced conditions, like plasma membrane CD38 which, however, also forms dimers and tetramers. Detection of cross-reactive epitopes was excluded by the use of a panel of anti-CD38 mAbs that recognize different epitopes. Nuclear CD38 maintains the enzymatic characteristics of the plasma membrane form, as shown by the production of cGDPR from the substrate NGD^+. This indicates that nuclear CD38 is enzymatically active.

Another finding of this study is that the plasma membrane and nuclear pools of CD38 are differentially regulated. Pharmacological agents known to be potent inducers of surface CD38 failed to induce any detectable modifications in nuclear CD38. The observation that the nuclear pool of CD38 is constitutive and independent from the plasma membrane CD38 pool suggests that after glycosylation, the rough ER may direct a protein to a particular location within the nuclear or/and plasma membrane compartments. The consequences are that: (i) CD38 does not migrate from the plasma membrane to the nucleus, explaining why the two CD38 pools are neither proportional nor related and (ii) nuclear import from the ER enables proteins which lack a nuclear signal sequence, such as CD38, to reach the nucleus. A possible pathway may lead glycosylated CD38 through the ER to the perinuclear cisterns and then to the inner nuclear membrane. From there, CD38 may migrate to the nucleus. This path is reported to be followed by CD38 in non-hemopoietic cells [Khoo et al., 2000]. In consequence of its dual localization, CD38 may perform as yet unknown location-specific functions. It is also reasonable to predict that each subcellular pool of CD38 may be differently regulated.

Evidence supporting the idea of distinct pools of CD38 is provided by Munoz et al. [2008] who recently showed that CD38 is part of the immunological synapse in human T lymphocytes. Interestingly, the CD38 molecules seen converging towards the synapse came from the surface pool and—unexpectedly—from an internal pool.

In summary, the characterization of a nuclear form further enhances the versatility of CD38 which is not only a dual-function but also a dual-localization protein.

ACKNOWLEDGMENTS

This study was supported by the Università Politecnica delle Marche Research Grant (2008) to RDP.

REFERENCES

Adebanjo OA, Anandatheerthavarada HK, Koval AP, Moonga BS, Biswas G, Sun L, Sodam BR, Bevis PJ, Huang CL, Epstein S, Lai FA, Avadhani NG, Zaidi M. 1999. A new function for CD38/ADP-ribosyl cyclase in nuclear Ca2+ homeostasis. Nat Cell Biol 1:409–414.

Adebanjo OA, Koval A, Moonga BS, Wu XB, Yao S, Bevis PJ, Kumegawa M, Zaidi M, Sun L. 2000. Molecular cloning, expression, and functional characterization of a novel member of the CD38 family of ADP-ribosyl cyclases. Biochem Biophys Res Commun 273:884–889.

Ausiello CM, Urbani F, Lande R, la Sala A, Di Carlo B, Baj G, Surico N, Hilgers J, Deaglio S, Funaro A, Malavasi F. 2000. Functional topography of discrete domains of human CD38. Tissue Antigens 56:539–547.

Di Pietro R, Santavenere E, Centurione L, Stoppia L, Centurione MA, Vitale M, Rana R. 1997. TNF-alpha-induced apoptosis in Daudi cells: Multiparametric analysis. Cytokine 9:463–470.

Drach J, Zhao S, Malavasi F, Mehta K. 1993. Rapid induction of CD38 antigen on myeloid leukemia cells by all trans-retinoic acid. Biochem Biophys Res Commun 195:545–550.

Dundr M, Hebert MD, Karpova TS, Stanek D, Xu H, Shpargel KB, Meierm UT, Neugebauer KM, Matera AG, Misteli T. 2004. In vivo kinetics of Cajal body components. J Cell Biochem 164:831–842.

Ferrero E, Orciani M, Vacca P, Ortolan E, Crovella S, Titti F, Saccucci F, Malavasi F. 2004. Characterization and phylogenetic epitope mapping of CD38 ADPR cyclase in the cynomolgus macaque. BMC Immunol 21: 5–21.

Ferrero E, Saccucci F, Malavasi F. 1999. The human CD38 gene: Polymorphism, CpG island, and linkage to the CD157 (BST-1)gene. Immunogenetics 49:597–604.

Funaro A, Spagnoli GC, Ausiello CM, Alessio M, Roggero S, Delia D, Zaccolo M, Malavasi F. 1990. Involvement of the multilineage CD38 molecule in a unique pathway of cell activation and proliferation. J Immunol 145:2390–2396.

Gall JG. 2003. The centennial of the Cajal body. Nat Rev Mol Cell Biol 4:975–980.

Grynkiewicz G, Poenie M, Tsien RY. 1985. A new generation of Ca2+ indicators with greatly improved fluorescence properties. J Biol Chem 260:3440–3450.

Hirata Y, Kimura N, Sato K, Ohsugi Y, Takasawa S, Okamoto H, Ishikawa J, Kaisho T, Ishihara K, Hirano T. 1994. ADP ribosyl cyclase activity of a novel bone marrow stromal cell surface molecule, BST-1. FEBS Lett 356:244–248.

Horenstein AL, Crivellin F, Funaro A, Said M, Malavasi F. 2003. Design and scaleup of downstream processing of monoclonal antibodies for cancer therapy: From research to clinical proof of principle. J Immunol Methods 275:99–112.

Hoshino S, Kukimoto I, Kontani K, Inoue S, Kanda Y, Malavasi F, Katada T. 1997. Mapping of the catalytic and epitopic sites of human CD38/NAD+ glycohydrolase to a functional domain in the carboxyl terminus. J Immunol 158:741–747.

Katz F, Povey S, Parkar M, Schneider C, Sutherland R, Stanley K, Solomon E, Greaves M. 1983. Chromosome assignment of monoclonal antibody-defined determinants on human leukemic cells. Eur J Immunol 13:1008–1013.

Khoo KM, Chang CF. 2002. Identification and characterization of nuclear CD38 in the rat spleen. Int J Biochem Cell Biol 34:43–54.

Khoo KM, Han MK, Park JB, Chae SW, Kim UH, Lee HC, Bay BH, Chang CF. 2000. Localization of the cyclic ADP-ribose-dependent calcium signaling pathway in hepatocyte nucleus. J Biol Chem 275:24807–24817.

Kishimoto H, Hoshino S, Ohori M, Kontani K, Nishina H, Suzawa M, Kato S, Katada T. 1998. Molecular mechanism of human CD38 gene expression by retinoic acid. Identification of retinoic acid response element in the first intron. J Biol Chem 273:15429–15434.

Kung P, Goldstein G, Reinherz EL, Schlossman SF. 1979. Monoclonal antibodies defining distinctive human T cell surface antigens. Science 206:347–349.

Lee HC. 1997. Mechanisms of calcium signaling by cyclic ADP-ribose and NAADP. Physiol Rev 77:1133–1164.

Lee HC. 2006. Structure and enzymatic functions of human CD38. Mol Med 12:317–323.

Lund FE. 2006. Signaling properties of CD38 in the mouse immune system: Enzyme-dependent and -independent roles in immunity. Mol Med 12:328–333.

Malavasi F, Deaglio S, Ferrero E, Funaro A, Rancho J, Ausiello CM, Ortolan E, Vaisitti T, Zubiaur M, Fedele G, Aydin S, Ribaldi EV, Duelli I, Lusso R, Cozno F, Horenstein AL. 2006. CD38 and CD157 as receptors of the immune system: A bridge between innate and adaptive immunity. Mol Med 12:334–341.

Munoz P, Mittelbrunn M, de la Fuente H, Perez-Martinez M, Garcia-Perez A, Ariza-Veguillas A, Malavasi F, Zubiaur M, Sánchez-Madrid F, Sancho J. 2008. Antigen-induced clustering of surface CD38 and recruitment of intracellular CD38 to the immunological synapse . Blood 111:3653–3664.

Platani M, Lamond AI. 2004. Nuclear organization and subnuclear bodies. Prog Mol Subcell Biol 35:1–22.

Rao GHR. 1988. Measurement of ionized calcium in normal human blood platelets. Anal Biochem 169:400–404.

Shimizu T, Pommier Y. 1997. Camptothecin-induced apoptosis in p53-null human leukemia HL60 cells and their isolated nuclei: Effects of the protease inhibitors Z-VAD-fmk and dichloroisocoumarin suggest an involvement of both caspases and serine proteases. Leukemia 11:1238–1244.

Trubiani O, De Fazio P, Pieri C, Mazzanti L, Di Primio R. 2000. Nuclear matrix provides linkage sites for translocated NF-kappa B: Morphological evidence. Histochem Cell Biol 113:369–377.

Trubiani O, Guarnieri S, Eleuterio E, Di Giuseppe F, Orciani M, Angelucci S, Di Primio R. 2007. Insights into nuclear localization and dynamic association of CD38 in Raji and K562 cells. J Cell Biochem 103:1294–1308.

Trubiani O, Salvolini E, Staffolani R, Di Primio R, Mazzanti L. 2003. DMSO modifies structural and functional properties of RPMI-8402 cells by promoting programmed cell death. Int J Immunopathol Pharmacol 16:253–259.